Archives of Hydro-Engineering and Environmental Mechanics 70 (2023), pp. 49–69, doi: 10.2478/heem-2023-0004

sciendo

ARCHIVES OF HYDRO-ENGINEERING AND ENVIRONMENTAL MECHANICS

Published since 1954

ISSN 1231–3726

Numerical Analysis of Turbulent Flow over a Backward-facing Step in an Open Channel

Bala Kawa M. Saleem[1], Andam Mustafa[2,*], Dalshad Ahmed Kareem[3], Mehmet Ishak Yuce[4], Michał Szydłowski[2], Nadhir Al-Ansari[5]

[1]General Directorate of Water and Sewage, Ministry of Municipalities and Tourism, Erbil 44001, Iraq; bala.kawa@yahoo.com; [2]Faculty of Civil and Environmental Engineering, Gdańsk University of Technology, Narutowicza 11/12, Gdańsk 80–233, Poland; mszyd@pg.edu.pl; [3]Erbil Technology College, Erbil Polytechnic University, Erbil 44001, Iraq; dalshad.kareem@epu.edu.iq; [4]Department of Civil Engineering, Gaziantep University, Gaziantep 27310, Turkey; yuce@gantep.edu.tr; [5]Department of Civil, Environmental and Natural Resources Engineering, Lulea University of Technology, Lulea 971 87, Sweden. nadhir.alansari@ltu.se; *Corresponding Author: Andam Mustafa, andam.mustafa@pg.edu.pl

(Received 1 December 2022; revised 18 April 2023)

Abstract. Computational examinations of the flow field in an open channel having a single Backward-Facing Step (BFS) with a constant water depth of 1.5 m were performed. The effects of the expansion ratio, and the flow velocity along the reattachment length, were investigated by employing two different expansion ratios of 1.5 and 2, and eight various flow velocities of 0.5, 1, 2, 3, 4, 5, 7.5 and 10 m/sec in the Computational Fluid Dynamic (CFD) simulations. Commercially available CFD software, ANSYS FLUENT, was used for calculations. The simulation outcomes were verified using experimental results. Moreover, analyses were performed by using two equation turbulence closure models, K-ε family (standard, RNG and realizable), and K-ω family (Wilcox's and SST K-ω). The analyses have revealed that the reattachment length increases with an increase in the expansion ratio, the flow velocity and the Reynolds number. The results obtained for two expansion rates and eight different flow velocities have shown insignificant differences between one turbulence closure model and the others. Furthermore, it was observed that both velocity and expansion ratios have an effect on the reattachment zone size.

Key words: open channel, backward-facing step, reattachment length, expansion ratio, K-ε model, K-ω model

1. Introduction

In water management, an open channel is defined as a man-made channel with a free surface that is constructed on the ground to transfer water from a river, another channel, a reservoir, or another storage area to a consumption point. In practice, the design of an ideal open channel lateral cross-section and longitudinal profile that meets all of the desired objectives is extremely difficult. There are several reasons for this: first,

there are many interdependent variables involved throughout the process, and second, there are many constraints that are commonly encountered within the area in question (Mustafa 2012). One of the main geometrical issues in open channels is the sudden change in the bed profile of the channel. If the bed of the channel has a downward step, an isolation and separation zone take place in the water stream, which is characterized by a Backward-Facing Step (BFS). Flow over a downward-stepping creates a recirculation zone where the fluid separates and forms vortices. Separation is a phenomenon that arises under a variety of flow conditions. Flow separation results from a strong adverse pressure gradient due to a sudden expansion in the geometry. The reattachment point is defined as the point where the flow contacts the base of the channel, while the reattachment length is known as the distance from the step to the reattachment point. The reattachment length is noted to vary from 5 step-heights to 8 step-heights depending upon the flow conditions (Saad 2011). Interest in the inflow over backward facing steps and reattachment length was revived in the early 1980s by employing laminar, turbulent and transitional flow conditions and different expansion ratios (Armaly et al 1983, Barri et al 2010; Benedict, Gould 1998, Durst, Tropea 1981, Eaton, Johnston 1981, Lee, Mateescu 1998, Panjwani et al 2009). Flows in BFS geometry are important due to the fact that flow separation substantially increases the momentum, heat, and mass transfer downstream of the step (Zajec et al 2021). Further development and validation of numerical turbulence flow methods are still required, due to the complexity of turbulence itself.

In an experimental study, Durst and Tropea (1981) explored the effect of the Expansion Ratio (ER) and Reynolds number for the reattachment length. They discovered that the length of the reattachment increases as the ER and Reynolds number increase. The experiments were performed with an ER = 20, which was similar to that of Kim et al (1980), who used an ER = 16.6. Sinha et al (1981) experimentally analyzed both laminar and turbulent flows over backward-facing steps. The range of Reynolds numbers used for the experiments varied from 100 to 12500. It was determined that the reattachment length increases linearly in the laminar flow regime (until $Re = 800$), then decreases as the Reynolds number increases. The reattachment length reaches a constant value of around six step heights (6h) for $Re > 10000$. Armaly et al (1983) explored the effect of Reynolds number on the reattachment length. A range of Reynolds number values were tested with three different flow regimes, namely: laminar, transition, and turbulence. The flow over the steps showed signs of Two-Dimensional (2-D) behavior at very low and very high Reynolds numbers ($Re < 400$ and $Re > 6600$). While it was mainly Three-Dimensional (3-D) for Reynolds numbers in between those values. The study led to the conclusions that: (i) the reattachment length increases with low Reynolds number ($Re < 1200$); (ii) for the transitional flow regime; the reattachment length decreases slightly with ($1200 < Re < 6600$); and (iii) it reamins mostly the same in fully turbulent flow. This group of researchers have reached similar conclusions in previous studies (Armaly et al 1983, Durst, Tropea 1981, Sinha et al 1981). Benedict and Gould (1998) found the

reattachment length to be 6.38h (where h is height of the step) for a Reynolds number of Re = 23600, the expansion ratio of the channel was 1.25. Pont-Vílchez et al (2019) conducted research on the direct numerical simulation of BFS flow at a Reynolds number of 395 and an expansion ratio of 2. At moderate Reynolds numbers, Tihon et al (2012) investigated the BFS flow experimentally and numerically. Different channel expansion ratios (ER = 1.43, 2, 2.5, and 4) and inlet flow conditions (steady and pulsatile) were used to study the structure and stability of flow behind the step.

The reattachment point location varies in the span-wise direction, and it moves about a mean value of 6 ER. The results of Direct Numerical Simulation (DNS) are similar to the experimental results. The DNS simulations show a large negative skin friction in the recirculation region at relatively low Re similar with the experimental result. Furthermore, the velocity profiles deviate from the log law in the recirculation zone. This presents that the flow is not fully recovered even at twenty step heights behind the down-step (Biswas et al 2004, Jovic, Driver 1994, Krishnamoorthy 2007, Le et al 1997, Neumann, Wengle 2003).

The pressure losses increase with increasing step height and decrease with increasing Reynolds number, except for $Re > 200$ and large expansion ratios. The 3-D prediction at three different Reynolds numbers (Re = 397, 648 and 800) were found to be in excellent agreement with the experimental results of (Armaly et al 1983). The effect of the side wall is evident for $Re > 400$, explaining the disagreements observed between 2-D simulations and the experimental findings in the vertical mid-plane. In contrast to the remarks of Kaiktsis et al (1991), an oscillatory behavior of the BFS flow was found beyond $Re \approx 1200$, which is in concurrence with the measurements of (Armaly et al 1983, Estejab 2011). Qingfu and Zhiping (2012) have investigated flow the relationship between the reattachment length, step height, flow depth on the step and the velocity on the step by applying two-phase numerical simulation by combining Volume-of-Fluid (VOF) method with Renormalizing Group (RNG) K-ε turbulence closure model. Numerical simulation results concluded that the reattachment length does not change with the flow velocity on the step. A quadratic relationship between the ratio of reattachment length and the step height was noted (Chanson 2004, Qingfu, Zhiping 2012).

Turbulence closure models of one equation to higher order ones have been employed in the calculation of reattachment length and BFSs. Anwar-ul-Haque et al (2007) had studied turbulence models for flow over BFSs and performed predictions for reattachment length with different turbulence closure models in 2-D and 3-D. Determination of reattachment length of separated shear layers in low Reynolds number turbulent flow is an important consideration to evaluate the quality of various turbulence models. Choi and Nguyen (2016) investigated the numerical BFS flow over a variety of step angles; the outcomes have been confirmed that the reattachment length remains almost constant once $Re > 15000$, even increasing of the step angle larger than 30 degrees. Araujo and Rezende (2017) presented and analyzed the turbulent flow in a 2-D channel with a BFS using numerical simulations. When they compared

to published results for reattachment length, mean velocity profile, and contour, the SST K-ω model produced the best results for reattachment length, mean velocity profile, and contour. When compared to models of two partial differential equations that employ the Boussinesq hypothesis, the Reynolds Stress Model (RSM) produced the best results for the turbulence intensity profile (Araujo, Rezende 2017).

The Large-Eddy Simulation (LES), which was initially conceived of by Smagorinsky (1963) and Lilly (1966), implicitly calculates the large-scale vortices and explicitly parameterizes the small-scale vortices. The LES can detect large scale vortex motion although with a larger grid-grid cell size, more over LES model tends to overestimate the tope wall separation, and the Reynolds stress components for the BFS flow simulation without a sufficiently fine grid, overall, LES is a potential tool for simulating separate flow controlled by large scale vortices (Wang et al 2019). The impact of grid resolution and sub-grid scale modeling on the predictive accuracy of LES is investigated (Shehadi 2018). Different combinations of streamwise and spanwise grid resolutions are considered along with different strategies for the cell-size distribution in the wall-normal direction.

In spite of the numerous numerical studies using turbulence models, there has been little research in the BFS area with considering different flow velocities and using different turbulence closure models, K-ε family (standard, RNG and realizable), and K-ω family (Wilcox's and SST K-ω). Currently, there is still a lack of numerical data reporting BFS flow behaviour at higher Reynolds numbers, which is necessary because the effects of low Reynolds numbers are mitigated at these levels. In the current research, numerical analyses were performed in order to look at the flow field over BSFs and the reattachment length for different Reynolds numbers. Two different expansion ratios of 1.5 and 2, and eight different flow velocities were employed using computational fluid dynamic (CFD) simulations. This research was conducted with the goals of determining the predictive ability of the various models for the BFS.

2. Material and Methods

2.1. Computational Domain Geometry

The view of the BFS flow domain analyzed in this research is shown in Figure 1. The expansion ratios are ER = Hd / (Hd $-h$) = 2 and 1.5, with aspect ratios equal to A_r = W/h = 6 and 4 (h = 0.5 and 0.75 m), where Hd is water depth in downstream of the step, W is the width of the channel, and h is the height of step. The computational domain has a total length 15 m. The height of step h is equal to 0.5 m and 0.75 m, length of upstream LU is 5 m and downstream length LD is 10 m).

For an ER of 1.5 m, the mesh that was constructed for the investigation of the flow field over the BFS in this study has 480 000 elements and 508 191 nodes. On the other hand, the mesh that was created for an expansion ratio of 2 contains a total of 450 000 elements and 477 691 nodes. In the meshing, 7 face zones and 1 cell zone were determined in order to resolve the boundary layer. Maximum face size of

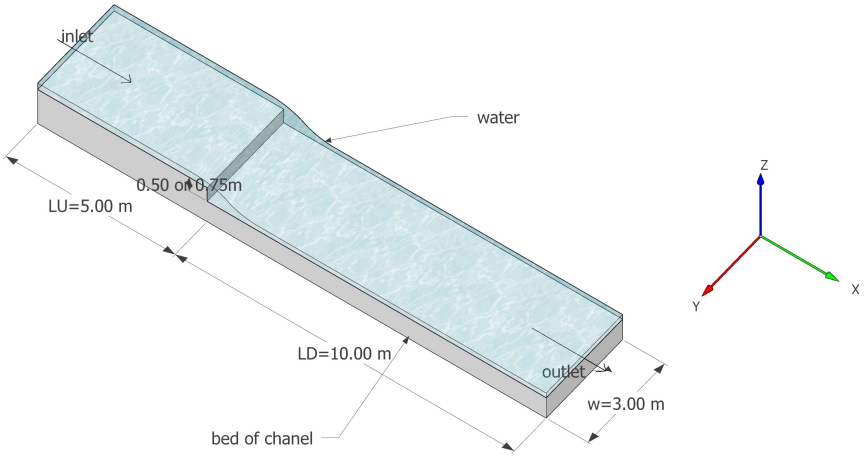

Fig. 1. Model layout

the mesh was assumed to be 0.0025 m^2. The orthogonal quality ranges from 0 to 1, where values close to 0 correspond to low quality. The minimum orthogonal quality of the present mesh is equal to 1 and maximum aspect ratio is 1.73.

Numerical analyses were performed to investigate the flow field over backward-facing steps and reattachment length for different Reynolds numbers. The range of Reynolds number used for this investigation varied for ER = 1.5 from 332 to 6646.72, and for ER = 2 it varied from 498.5 to 9970.08. The effects of the flow velocity along the reattachment length were investigated by employing eight different flow velocities of 0.5, 1, 2, 3, 4, 5, 7.5 and 10 m/sec in the CFD simulations. Simulations were performed by using five different turbulence closure models, namely, standard K-ε, RNG K-ε, realizable K-ε, Wilcox's K-ω and SST K-ω (Launder and Spalding 1972, Menter 1994, Shih et al 1995, Wilcox 1998, Yakhot, Orszag 1986). The analyses were conducted by employing commercially available CFD software, ANSYS FLUENT. The reattachment length is found to vary from 5 step-heights to 8 step-heights, depending on the flow conditions (Yüce 2005).

2.2. Turbulence Models

In a physical domain, the Navier-Stokes equations mathematically depict the balance of momentum and conservation of mass for Newtonian fluids. These equations may be accompanied by an equation of state that establishes the relationship between pressure, temperature, and density of the fluid. They are derived from the application of Isaac Newton's second law to fluid motion, assuming that the stress within the

fluid consists of two components: a diffusing viscous term, which is proportional to the velocity gradient, and a pressure term. This description enables the characterization of viscous flow in fluids. When attempting to obtain accurate results by the use of the Reynolds averaging, application of turbulence models is absolutely necessary (Yakhot, Orszag 1986).

The Standard k-ε (SKE) model is the most commonly used of the two-equation turbulent models. The model solves two further differential equations for kinetic energy, k and dissipation ε (Launder, Spalding 1972). The standard k-ω (SKO) model is a two-equation linear eddy viscosity turbulence model which was developed by Wilcox (1998) and it is known by that name. Wilcox has referred to specific dissipation rate, ω, as the ratio of ε to k. In another word, it is a rate of dissipation per unit kinetic energy. The SKO model can be applied to both walls bounded flows and shear flows. The model also incorporates specific changes that include low Reynolds number effects. The shear stress transport (SST) k-ω model was developed by Menter (1994). In this study, the SKO model is applied in the near wall regions whereas the SKE model is incorporated in the free-stream region of the flow. This is done by converting the SKE model to a SKO model in the near wall region. A blending function is multiplied to both the models which are then added together. The function has a value of '1' near the wall, thereby activating SKO model, and a value of '0' far away from the wall, which triggers the SKE model. These attributes make the SST model more accurate and reliable than the SKO model (Gerasimov 2006, Sobieski 2013).

2.3. Boundary Conditions

The inclusion of boundary conditions has the potential to have a significant impact, both on the precision and the convergence of the solution. During the problem setup phase, after selecting and defining the boundary condition, particle flow properties will need to be specified. In this work a total of six boundary conditions is considered, of which the three are the most significant ones. The boundary conditions that were applied to the current geometry are listed in Table 1.

Table 1. Model boundary conditions

Zone	Type
Inlet	Pressure inlet (barometric, elevation of water surface = 1.5 m)
Outlet	Pressure outlet (barometric)
Surface	Wall-free slip with air
Side wall	Wall-no slip
Bottom	Wall-no slip

The pressure inlet and pressure outlet boundary condition specify the inlet velocity in m/sec and the outlet velocity. The outlet velocity requires the specification of a length scale such as the hydraulic diameter of the inlet channel and the turbulent intensity. FLUENT provides a default value of 10% turbulent intensity; however,

the turbulence intensity and length scale can be specified by the user. A turbulence intensity of 1% or less is generally used for flows with low Reynolds numbers and turbulence intensities greater than 10% are used for high Reynolds number flows. The intensity can be determined by using:

$$I = 0.16(R_e)^{-1/8}. \tag{1}$$

The turbulence length scale is a physical quantity related to the size which can be defined by:

$$\ell = 0.07L. \tag{2}$$

In non-circular cross-sectional open channel flows, L is based on the hydraulic diameter of the channel. Velocity in this work was selected by choosing multiphase option in pressure inlet and filling the field for velocity magnitude and the bottom of the bed with surface water in open channel. The same choice is used to implement turbulence intensity and length scale ratio, and to select the bottom of the bed with surface water multiphase. For both side-walls and the bottom boundary the no slip condition was defined. The surface boundary condition was chosen to be the wall in type with a free-slip shear condition.

Pressure-velocity coupling method and spatial discretization ought to be defined in the solution stage, which is necessary for obtaining accurate results. The pressure-velocity coupling method consists of SIMPLE, SIMPLEC and PISO algorithms. Applying the pressure-based segregated algorithm indicates that the pressure--based coupled solver is used. Corrected velocity and pressure fields represent a high approximated relationship in Pressure Implicit with Splitting Operators (PISO) algorithm, especially applicable to transient problems, which can improve the convergence in highly distorted cells. The first order segregated upwind solver is stable but dissipative, depending on the direction of flow. On the other hand, the second order upwind scheme does not depend on the flow direction; it is symmetric and not dissipative, but dispersive. The third order quadratic upwind interpolation for convection kinetics (QUICK) is used only for hexagonal and quadrate pressure interpolation scheme (pressure at the cell-faces). QUICK depends on the flow direction.

The numerical solution of the flow field was performed by choosing standard initialization method. All values under the initial values heading are automatically computed and updated based on the conditions defined at the selected boundary zone. One or more of the default values can be changed or new values could be input, usually in the fields next to the current variables. The last step in the solution stage is to estimate the current data by running the calculation task. The details of the calculation run depend on the steady-state analyzing and performing time-dependent computation according to the requirements. For example, if the eddy simulation is being analyzed the transit time must be enabled in general setup task. The present study did not need

transit time, since it works with k-ε and k-ω turbulence closure models and steady flow condition. The number of iteration and time step can be defined prior to execution.

3. Results and Discussion

The results obtained in this research for the reattachment length were compared with experimental and numerical analyses available in the literature. The flow behind the BFSs produces recirculation zones, where the fluid separates and forms vortices. The analyses have revealed that the reattachment length increases with an increase in the ER, the flow velocity and, thus, the Reynolds number. Table 2 presents the naming order of simulated scenarios.

Table 2. The naming of simulated scenarios in this study

Turbulence closure models		Velocity (m/sec)	Expansion ratio
K-ε	Standard K-ε RNGK-ε Realizable K-ε		1.5
K-ω	Standard K-ω SST K-ω	0.5, 1, 2, 3, 4, 5, 7.5, 10	
K-ε	Standard K-ε RNGK-ε Realizable K-ε		2
K-ω	Standard K-ω SST K-ω		

3.1. Flow over a Backward-facing Step with the Expansion Ratio of 1.5

The 2-D plots of velocity vector field and streamlines with contour for the ER = 1.5 are presented in Figures 2 and 3. The results of the study for the same expansion ratio are summarized in Table 3. The standard K-ε, renormalized group (RNG) K-ε, realizable K-ε, Wilcox k-ω, and shear stress transport (SST) K-ω turbulence closure models with Reynolds numbers ranging from 332 to 6646.72 were simulated. One of the important characteristics of the flow over BFSs is the recirculation region formed behind the step. The shear layer separates from the top of the step and reattaches to the bed of the expanded channel after the step at the reattachment point. In a numerical investigation conducted by Qingfu and Zhiping (2012), with an expansion ratio of 1.5, the reattachment length was measured to be varying between 5.1h and 4.9h. The reattachment length was observed to be fluctuating between 4.4h to 5.3h in an experimental study performed by Yüce (2005).

In the present research, it was found that the reattachment length varies from 4.4h to 5.98h for all K-ε nd K-ω turbulence models. The results of the analyses show that the reattachment length fluctuates from 4.68h to 5.88h, 4.4h to 5.89h, 4.54h to 5.8h, 4.5h to 5.8h, 4.7h to 5.98h for the standard K-ε, the RNG K-ε, Realizable K-ε, Wilcox

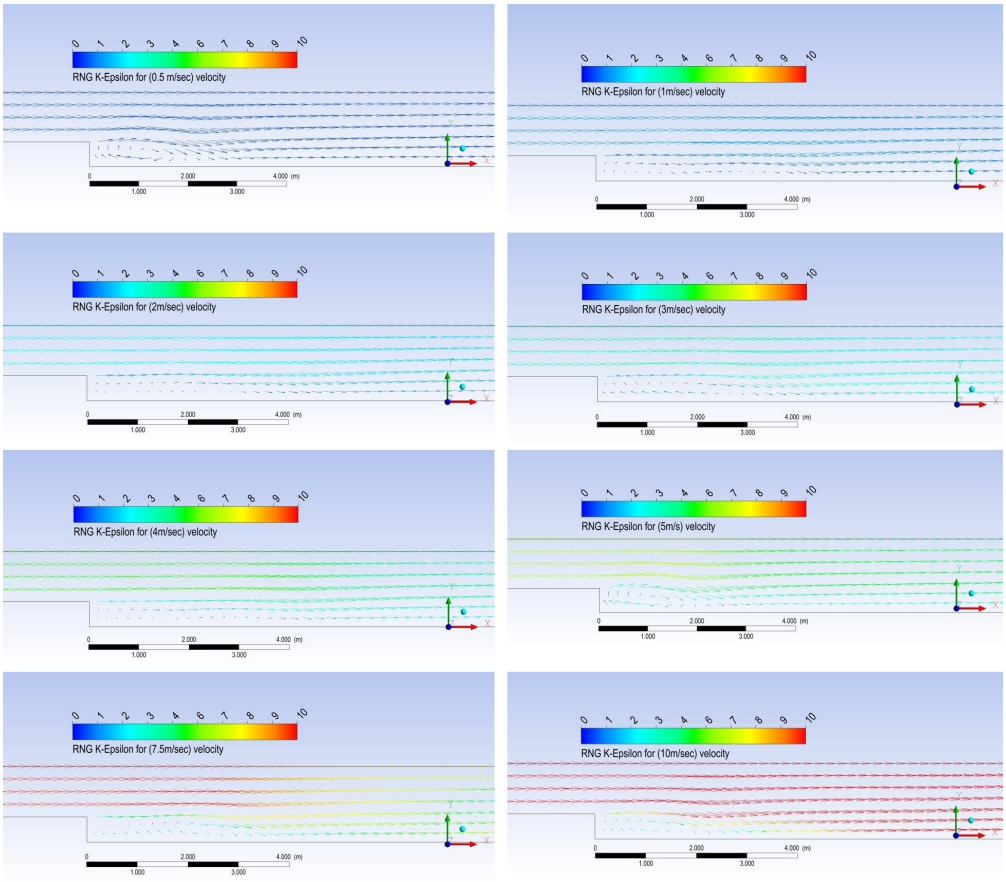

Fig. 2. Velocity vector with vortices for different values of Reynolds number for RNG K-ε model

k-ω, SST K-ω turbulence closure models, respectively. In comparison to the other models, the SST predicts the longest reattachment length when the velocity is set to 10 m/sec and Re = 6646.72. Standard and RNG K-ε almost have the same reattachment length, which equals 5.88 m. Finally, the minimum reattachment length was obtained by using Realizable K-ε as well as Standard K-ω. When the velocity is increased from 0.5 to 1 m/sec, and subsequently to 2, 3, 4, and 5 m/sec, then there is a correlation in the amount of increase in reattachment length; however, when the velocity is increased to 7.5 m/sec, the amount of increase in reattachment length is not the same as it was previously. When comparing to the experimental results obtained by (Yüce 2005) RNG, Realizable K-ε, Standard K-ω, and SST, the reattachment length is found to be in the range of the experimental study when the velocities are 0.5, 1, 2, 3 and 4 m/sec; thereafter, the reattachment length was greater than in the range. However, according to the S K-ε equation, the length will begin to be greater than the range of the experimental study after exceeding the velocity of 2 m/sec.

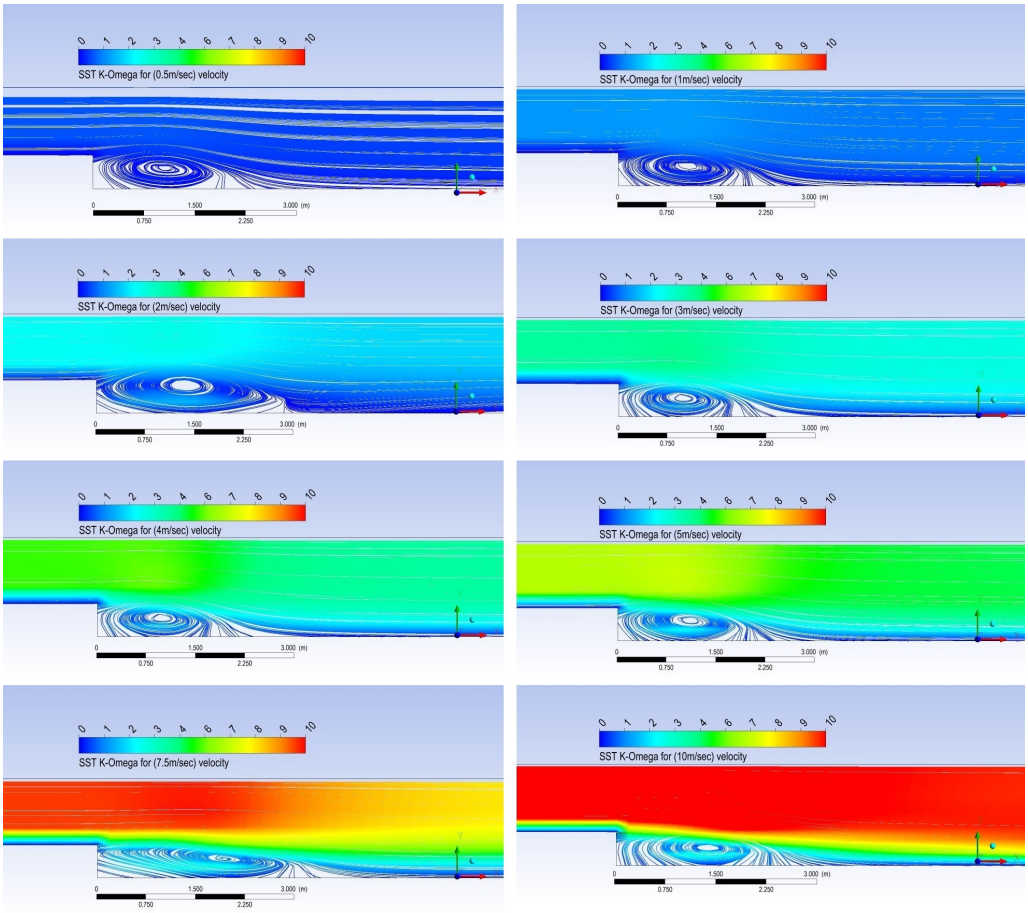

Fig. 3. Velocity contour for different values of velocity for SST K-ω model

The vortices in the shear layer of flows with a high Reynolds number were noted to shed more rapidly than those of low Reynolds numbers while approaching to the reattachment point. The re-circulation region was clearly distinguished and noticed to cover almost all of the downward area, with its center point slightly shifted towards the downstream for some models (Figures 2 and 3 and Table 3).

3.2. Flow over a Backward-facing Step with the Expansion Ratio of 2

The 2-D plots of velocity vector field and streamlines with contour for the expansion ratio of 2 are presented in Figures 4 and 5. The results of the study for the expansion ratio of 2 are summarized in Table 4. Analyses were performed by the standard K-ε, renormalize group (RNG) K-ε, realizable K-ε, Wilcox K-ω and shear stress transport (SST) K-ω turbulence closure models, with the Reynolds numbers ranging from 498.5 to 9970. One of the significant features of the flows over BFSs is the recirculation area

Table 3. Reattachment lengths for ER of 1.5 with 0.5 m step for k-ε and k-ω turbulence models

Re	V (m/sec)	Model					
		S K-ε	RNG	R K-ε	S K-ω	SST	Experimental
332.00	0.5	4.68	4.40	4.54	4.50	4.70	(4.4–5.3)
664.00	1	4.72	4.80	4.84	4.56	4.74	(4.4–5.3)
1329.01	2	5.22	4.96	4.92	4.82	4.76	(4.4–5.3)
1994.017	3	5.34	5.14	5.08	5.04	4.98	(4.4–5.3)
2685.025	4	5.50	5.26	5.30	5.16	5.24	(4.4–5.3)
3323.03	5	5.52	5.60	5.60	5.39	5.40	(4.4–5.3)
4985.04	7.5	5.60	5.62	5.62	5.40	5.56	(4.4–5.3)
6646.72	10	5.88	5.89	5.80	5.80	5.98	(4.4–5.3)

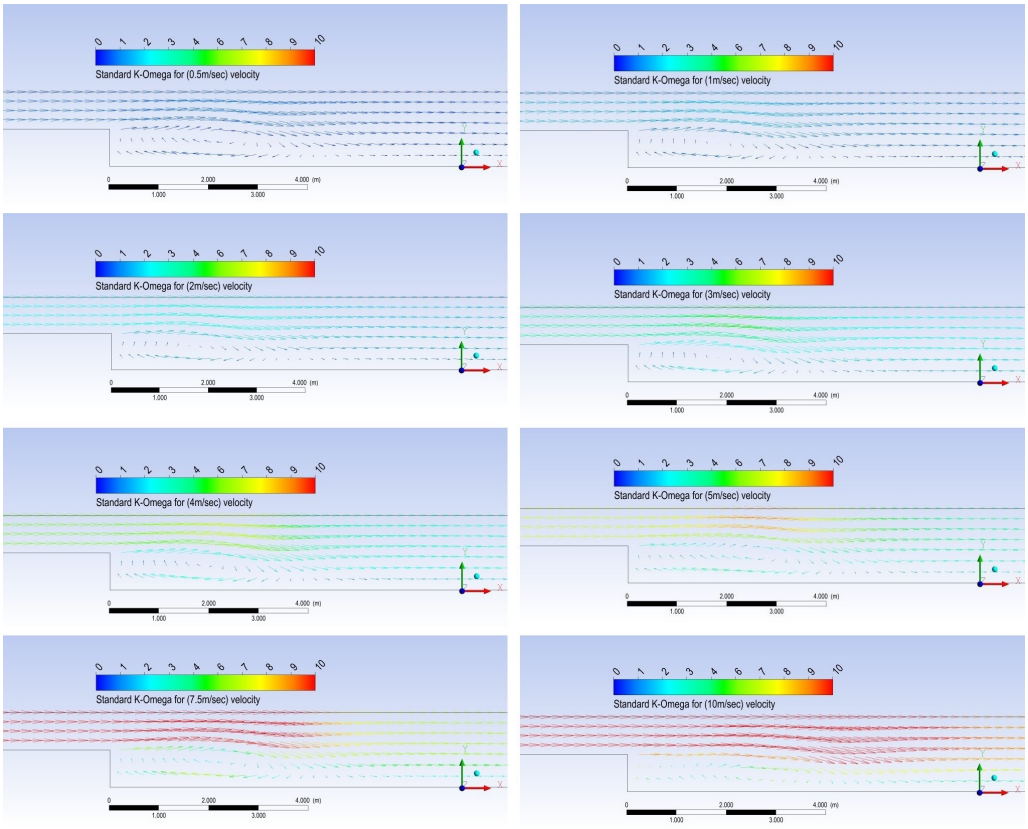

Fig. 4. Velocity vector with vortices for different values of Reynolds number for Wilcox K-ε model

developing just after the step. The shear layer separates from the top of the step and reattaches to the bed of the expanded channel after the step.

Qingfu and Zhiping (2012) stated that the reattachment length for the expansion ratio of 2 varies between 5.9h and 6.3h. In the experimental study conducted by Ar-

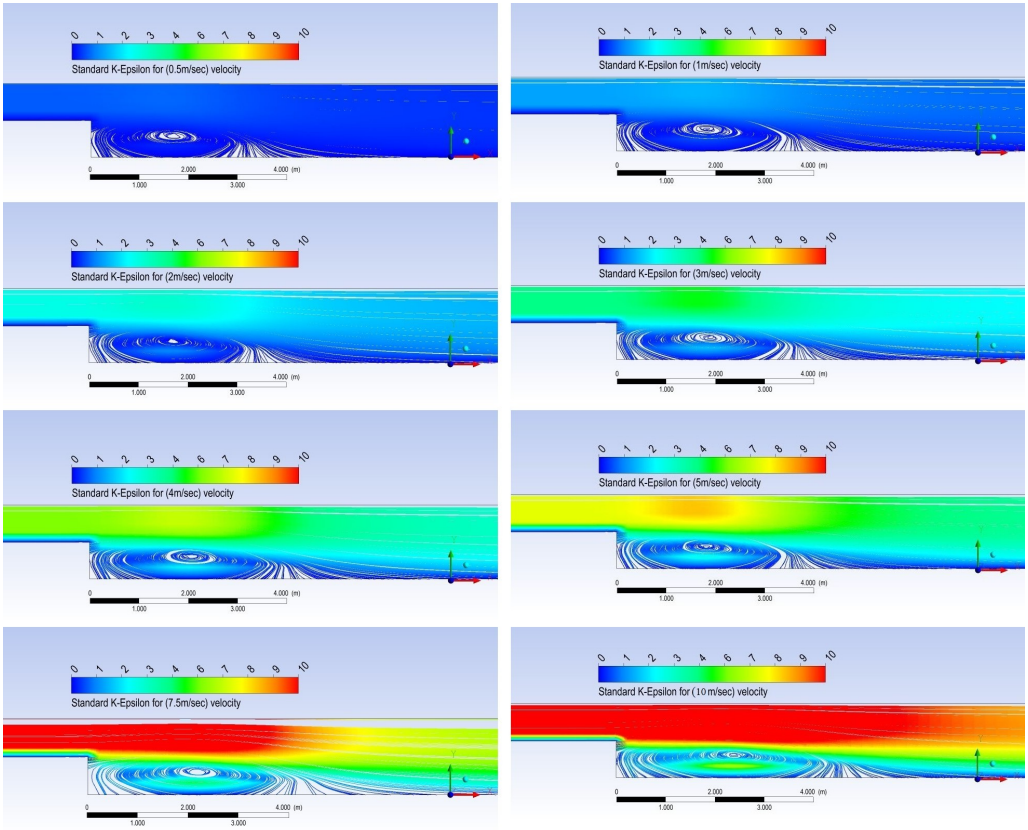

Fig. 5. Velocity contour for different values of velocity for standard K-ε model

maly et al (1983), for an expansion ratio of 2, with Reynolds number ranging from 7000 to 11400, it was found that the reattachment length ranges from 5.6h to 7.01h. The average reattachment length was noted by a number of researchers to be changing between 7.21h to 8h for the flow with an expansion ratio of 2. Sinha et al (1981) investigated the reattachment length for a turbulent flow over a BFS for different step angles. The reattachment length was observed to be around 6h for a 90° step with an expansion ratio of 2. In this study, it was found that the reattachment length ranges from 5.6h to 8h (Table 4).

The results of the numerical simulations demonstrate that the reattachment length varies from 5.67h to 8h, 5.73h to 7.87h, 5.72h to 7.8h, 5.65h to 7.6h, 5.6h to 7.87h for the standard K-ε, the RNG K-ε, Realizable K-ε, Wilcox k-ω, SST K-ω turbulence closure models, respectively. In comparison to the other models, the S K-ε and R K-ε predicts the longest reattachment length when the velocity is set to 10 m/sec and Re = 9970.08. SST and RNG K-ε have the same reattachment length, which equals 7.87 m. Finally, the minimum reattachment length was computed by using S K-ω.

Table 4. Reattachment lengths for ER = 2 with 0.75 m step for k-ε and k-ω turbulence models

Re	V (m/sec)	Model					
		S K-ε	RNG	R K-ε	S K-ω	SST	Experimental
498.50	0.5	5.67	5.73	5.72	5.65	5.60	$\approx$ 7.21
996.01	1	5.84	5.79	5.87	5.87	5.92	$\approx$ 7.21
1993.50	2	5.87	6.04	6.07	6.16	6.21	$\approx$ 7.21
2991.02	3	5.89	6.33	6.36	6.37	6.35	$\approx$ 7.21
3988.04	4	6.13	6.40	6.53	6.45	6.48	$\approx$ 7.21
4984.50	5	6.80	6.67	6.80	6.53	6.65	$\approx$ 7.21
7477.50	7.5	7.01	7.33	7.20	7.20	7.20	$\approx$ 7.21
9970.08	10	8.00	7.87	7.80	7.60	7.87	$\approx$ 7.21

When the velocity is increased from 0.5 to 1 m/sec, and subsequently to 2, 3, 4, and 5 m/sec, then there is a correlation in the number of increases in reattachment length; however, when the velocity is increased further to 7.5 m/sec, the amount of increase in reattachment length is not the same as it was in former cases. When comparing to the experimental results obtained by (Yüce 2005), for all equations, the calculated reattachment length is found to be smaller than that measured in the experimental study when the velocity is smaller than 10 m/sec; thereafter, the reattachment length was greater than that in the former range.

The vortices in the shear layer of flows with high Reynolds number were observed to shed more swiftly than those at low Reynolds number when approaching the reattachment point. The re-circulation area was evidently different and perceived to cover almost the entire downward zone, with its center point slightly shifted in the downstream direction, for all five models (Figures 4 and 5 and Table 4). The free surface effect has a more significant impact on the flow quantities in the vicinity of the step when compared to the BFS in a closed channel. The free surface effects upon the flow become less significant as streamwise distance increases, and profiles begin to resemble one another (Ampadu-Mintah and Tachie 2012).

3.3. Velocity with Reattachment Length

The velocity of flow has significant effects on the reattachment length (Hossain et al 2013). As the inlet velocity increases, the reattachment length was observed to increase within a certain range. Linear trend lines were fitted to the graphs acquired from the correlation between the reattachment lengths and the average velocities of the flow for all turbulence closure models studied here. The coefficients of these straight lines confirm the dependence of the reattachment length on the flow velocity (Figures 6 and 7). The lines are defined in terms of two coefficients a and b by equation (3). The values of the coefficients in the equation (3), calculated for all turbulence models examined here, are presented in the Table 5. The coefficients a, expressing the slopes of the fitting lines, are all positive. This shows an increase in the reattachment length

with the average velocity of flow. The corresponding correlation coefficients of trend lines are presented in Table 6.

$$y = ax + b. \tag{3}$$

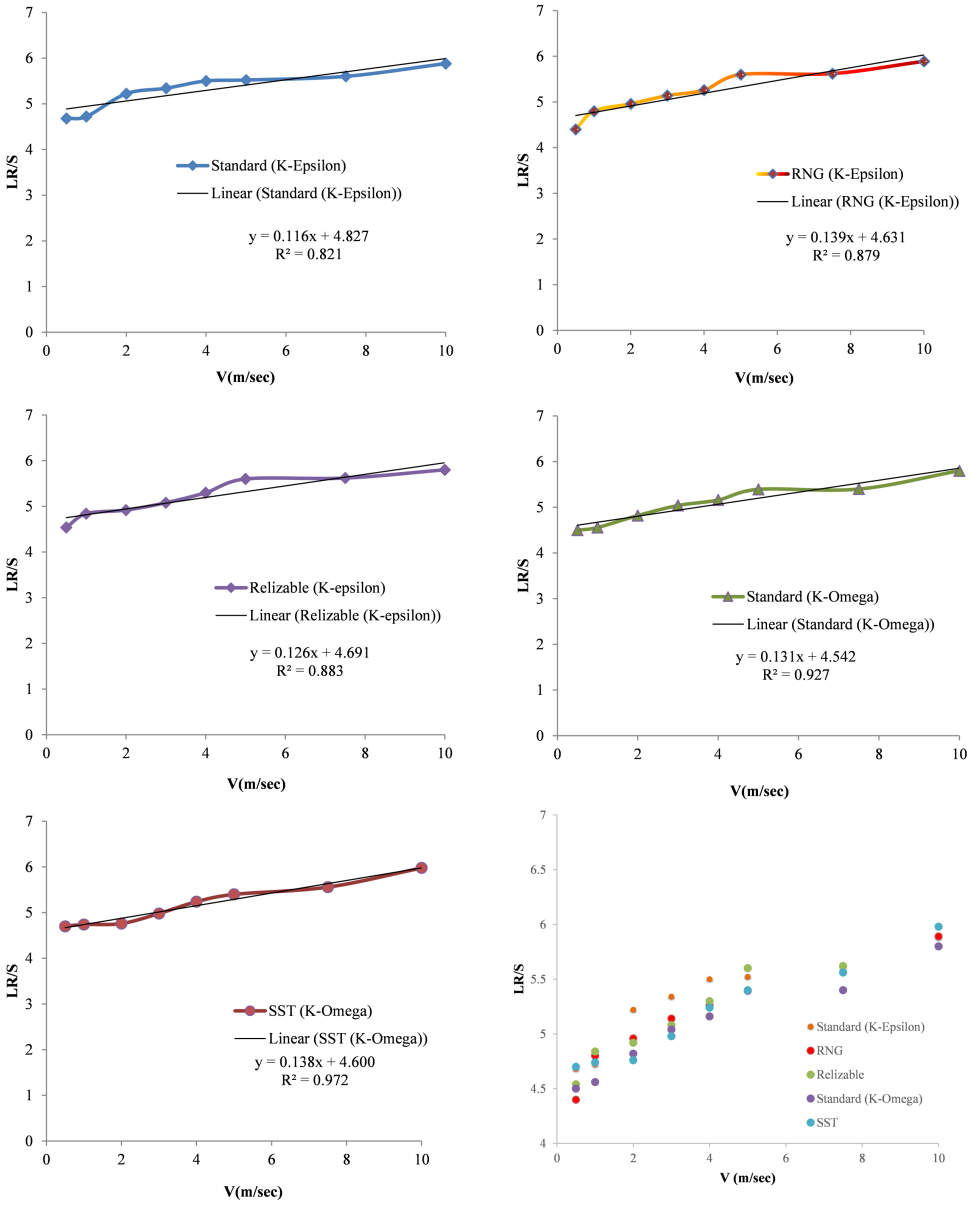

Fig. 6. Reattachment lengths for ER = 1.5 of K-ε and K-ω model

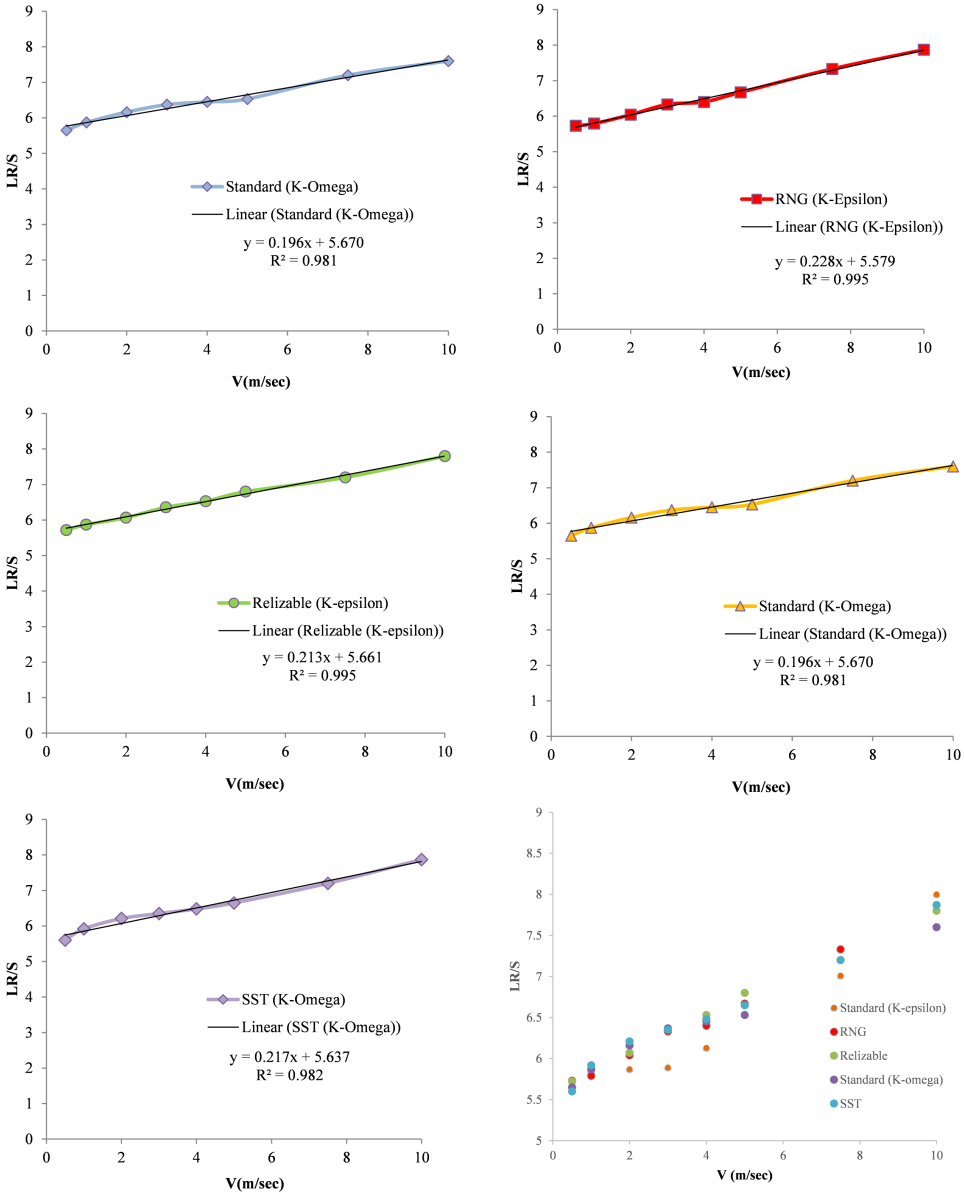

Fig. 7. Reattachment lengths for ER = 2 of K-ε and K-ω model

3.4. Expansion Ratio with Reattachment Length

The expansion ratio has a greater impact on reattachment and separation point than the velocity, as is shown in Figure 8. The constant b which denotes the starting point of the linear trend line fitted to the curves showing the relationship between the reattachment length and flow velocity, is equal to around 4.6 for the expansion ratio of 1.5, while it

Table 5. Coefficients and constants of the fitted trend linear lines

Re	ER = 1.5		ER = 1.5 2	
	a	*b*	*a*	*b*
STD K-ε	0.116	4.827	0.238	5.418
RNG K-ε	0.139	4.632	0.227	5.580
Realizable K-ε	0.126	4.691	0.214	5.659
STD K-ω	0.131	4.542	0.196	5.671
SST K-ω	0.138	4.601	0.217	5.638
Average	0.130	4.659	0.218	5.594

Table 6. Coefficients and constants of the fitted trend linear lines

Re	ER = 1.5		ER = 1.5 2	
	R^2	R	R^2	R
STD K-ε	0.821	0.906	0.939	0.969
RNG K-ε	0.879	0.937	0.995	0.997
Realizable K-ε	0.883	0.939	0.995	0.997
STD k-ω	0.928	0.963	0.981	0.991
SST k-ω	0.972	0.986	0.983	0.991
Average	0.897	0.946	0.979	0.980

is about 5.6 for the expansion ratio of 2. This shows an increase in the reattachment length with the increase in the expansion ratio.

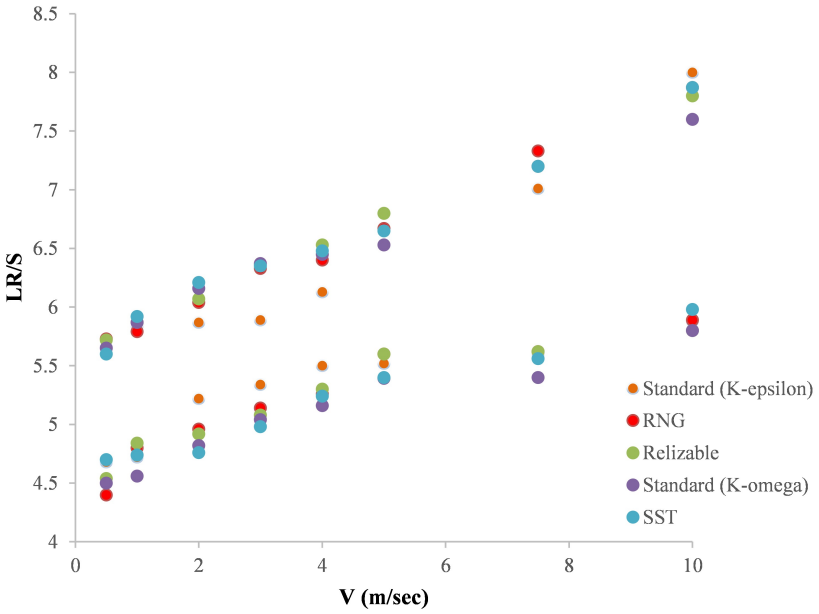

Fig. 8. Different types of K-ε and K-ω models, with 0.5 and 0.75 m step heights

3.5. Velocity Percentage

The values of the percentage of the average re-circulation velocity for the expansion ratio equal to 1.5 were noticed to be between 19.6 and 38.6% of the ambient stream velocity (immediate speed of water particle after the step), while the maximum re-circulation velocity was between 37 and 68.5% of the ambient velocity. The values of the percentage of the average re-circulation velocity for the expansion ratio equal to 2 were noticed to be between 20 and 37.5% of the ambient stream velocity, while the maximum re-circulation velocity was between 47.8 and 89% of the ambient velocity. Similar results have been obtained in (Yüce 2005). The velocity of water in the gyre is largest near the downstream of the step and decreases along the flow direction.

The formulation of the velocity percentage is given by equations (4) and (5). The coefficients of the equations for velocity percentage in all turbulence models employed here are presented in Tables 7, 8, 9 and 10. V_1 expresses the stream flow velocity, V_a is the average recirculation velocity, V_m is the maximum recirculation velocity, V_{Pa} is the percentage of the average recirculation velocity, and V_{Pm} is the percentage of the maximum recirculation velocity.

$$V_{Pa} = \frac{V_A}{V_1} \times 100, \tag{4}$$

$$V_{Pm} = \frac{V_m}{V_1} \times 100. \tag{5}$$

Table 7. Average re-circulation velocities and their percentage for ER of 1.5

ER	1.5									
V_1	Standard K-ε		RNG		Realizable		Standard k-ω		SST	
(m/sec)	V_A (m/sec)	V_{Pa} (%)	V_A	V_{Pa}	V_A	V_{Pa}	V_A	V_{Pa}	V_A	V_{Pa}
0.5	0.16	32.8	0.12	23.50	0.13	26.00	0.12	24.40	0.20	30.40
1	0.28	27.8	0.25	25.40	0.33	33.20	0.37	36.60	0.30	30.40
2	0.53	26.40	0.63	31.30	0.74	37.20	0.53	26.46	0.60	28.80
3	0.70	23.30	0.79	26.40	1.05	35.12	0.71	23.73	0.60	21.35
4	1.29	32.20	1.30	32.40	1.54	38.60	1.02	25.47	1.20	30.45
5	1.90	37.90	1.59	31.80	1.50	30.00	1.22	24.32	1.80	36.08
7.5	2.39	31.90	2.30	30.70	2.16	28.85	2.20	29.33	2.20	28.91
10	3.48	34.80	1.96	19.60	3.60	36.02	3.12	31.20	2.70	27.40

The formulation of the linear trend lines which were fitted to the graphs obtained by the correlation between the reattachment lengths and the average velocities of the flow is in the form of Eq. (6) and (7). The coefficients of these trend lines describe the dependence of the reattachment length on the flow velocity. The average value of the coefficient of x which expresses the slope of the fitting line is positive. This shows an increase in the reattachment length with the average velocity of the flow. Equation (6)

Table 8. Maximum re-circulation velocities and their percentage for ER of 1.5

ER	1.5									
V_1	Standard K-ε		RNG		Realizable		Standard k-ω		SST	
(m/sec)	V_m	V_{Pm} (%)	V_m	V_{Pm}	V_m	V_{Pm}	V_m	V_{Pm}	V_m	V_{Pm}
0.5	0.31	62	0.29	58	0.27	54	0.22	44	0.33	66
1	0.59	59	0.58	58	0.68	68	0.67	67	0.68	68
2	0.95	47.5	1.2	60	1.37	68.5	1.1	55.3	1.11	55.5
3	1.2	40	2.05	68.3	2.03	67.9	1.3	43.3	1.26	42
4	2.67	66.7	2.6	65	2.66	66.5	2.4	60	2.2	55
5	3.36	67.2	2.8	56	2.89	57.8	2.7	54	3.3	66
7.5	4.1	54.6	3.8	50.7	4.5	60	4.1	54.6	4.17	55.6
10	6.13	61.3	3.7	37	6.5	65	7.2	72	6.78	67.8

Table 9. Average re-circulation velocities and their percentage for ER of 2

ER	1.5									
V_1	Standard K-ε		RNG		Realizable		Standard k-ω		SST	
(m/sec)	V_A (m/sec)	V_{Pa} (%)	V_A	V_{Pa}	V_A	V_{Pa}	V_A	V_{Pa}	V_A	V_{Pa}
0.5	0.17	33.50	0.15	30.60	0.16	31.40	0.15	30.4	0.12	23.4
1	0.37	36.90	0.32	32.40	0.32	31.90	0.23	23.1	0.21	21.4
2	0.73	36.70	0.63	31.40	0.60	30.00	0.47	23.6	0.4	19.8
3	0.77	25.80	1.03	34.2	0.88	29.40	1.07	35.7	0.92	30.7
4	1.17	29.30	1.31	32.8	1.04	26.00	0.85	21.4	0.8	20
5	1.45	28.90	1.47	29.3	1.21	24.30	1.74	34.7	1.87	37.5
7.5	2.58	34.4	2.47	32.9	2.47	32.90	2.2	29.4	2.29	30.5
10	3.19	31.90	3.08	30.7	2.19	21.90	3.61	36.1	3.61	36.1

Table 10. Maximum re-circulation velocities and their percentage for ER of 2

ER	1.5									
V_1	Standard K-ε		RNG		Realizable		Standard k-ω		SST	
(m/sec)	V_m	V_{Pm} (%)	V_m	V_{Pm}	V_m	V_{Pm}	V_m	V_{Pm}	V_m	V_{Pm}
0.5	0.32	64	0.31	62	0.36	73.20	0.34	68.00	0.26	52.00
1	0.68	68	0.78	78	0.75	75.00	0.58	58.00	0.50	50.00
2	1.43	71.5	1.5	75	1.4	70.00	1.01	50.50	1.08	54.00
3	2	66.6	2.4	80	2.42	80.70	2.5	83.30	2.24	74.70
4	2.68	67	2.99	74.7	2.5	62.50	2.00	50.00	1.96	49.00
5	3.61	72.2	3.39	67.8	2.93	58.60	3.70	74.00	3.96	79.20
7.5	6.18	82.4	5.5	73.3	6.05	80.70	5.21	69.40	5.11	68.10
10	6.4	64	7.2	72	4.78	48.00	8.90	89.00	7.20	72.00

is the approximation for the expansion ratio of 1.5, when the expansion ratio of 2 is represented by Eq. (7).

$$y = 0.130x + 4.658, \tag{6}$$

$$y = 0.218x + 5.593. \tag{7}$$

If in equation (6), which is for ER = 1.5, the velocity value is included instead of x, then the reattachment point is obtained instead of being far from the step. And if in equation (7), which is for ER = 2, the velocity value is included instead of x, then the reattachment point is obtained instead of being far from the step.

4. Conclusions

Numerical simulations were performed for the flow field in an open channel having a single backward facing step with a constant water depth of 1.5 m. The effects of the expansion ratio and the flow velocity over the reattachment length are studied by adopting two different expansion ratios of 1.5 and 2, and eight different flow velocities of 0.5, 1, 2, 3, 4, 5, 7.5 and 10 m/sec. Analyses were performed by using five turbulence closure models, namely, the standard K-ε, RNG K-ε, Realizable K-ε, Wilcox's K-ω and SST k-ω. The commercial CFD software, ANSYS FLUENT, was employed for all the simulations. The results obtained from the simulations have revealed that the reattachment length increases with an increase in the expansion ratio, the flow velocity, and hence the Reynolds number. The results achieved for both expansion rates and eight different flow velocities have shown insignificant differences between one turbulence closure model and the others. Reynolds number ranged from 332 to 6646.72 for the expansion ratio of 1.5, while the range of Reynolds number was from 498.5 to 9970 for the expansion ratio of 2. The complexity of the backward-facing flow structure is increased when the expansion ratio is increased. It was noted that the reattachment length varies from 4.4h to 5.98h for the expansion ratio of 1.5, and it varies between 5.9h and 6.3h for the expansion ratio of 2. The recirculation zone expands as the velocity of the flow increases, but the amount of expansion is proportional to the velocity increase. After examining and comparing all of the turbulence closure models, we found that the Realizable K- model yields the results that are more effective and accurate than those given by the other models. The findings from this research can serve as a reference for engineering applications of numerical models that have limited computation capacity.

Data Availability Statement

The datasets generated during and/or analyzed during the current study are available from the corresponding author on reasonable request.

Conflict of Interest:

The authors declare that they have no conflict of interest.

Funding:

There was no funding source for this research.

References

Ampadu-Mintah A. A., Tachie M. F. (2012) Low Reynolds NumbfOpen Channel Flows Over a Backward Facing Step, *Fluids Engineering Division Summer Meeting: American Society of Mechanical Engineers*, 715–722.

Anwar-ul-Haque F. A., Yamada S., Chaudhry S. R. (2007) Assessment of turbulence models for turbulent flow over backward facing step, *Proceedings of the World Congress on Engineering*, 2–7.

Araujo P. P., Rezende A. L. T. (2017) Comparison of turbulence models in the flow over a backward--facing step, *International Journal of Engineering Research & Science*, **3**, 88–93.

Armaly B. F., Durst F., Pereira J., Schönung B. (1983) Experimental and theoretical investigation of backward-facing step flow, *Journal of fluid Mechanics*, **127**, 473–496.

Barri M., El Khoury G. K., Andersson H. I., Pettersen B. (2010) DNS of backward-facing step flow with fully turbulent inflow, *International Journal for Numerical Methods in Fluids*, **64**, 777–792.

Benedict L., Gould R. (1998) Concerning time and length scale estimates made from burst-mode LDA autocorrelation measurements, *Experiments in fluids*, **24**, 246–253.

Biswas G., Breuer M., Durst F. (2004) Backward-facing step flows for various expansion ratios at low and moderate Reynolds numbers, *J Fluids Eng*, **126**, 362–374.

Chanson H. (2004) *Hydraulics of open channel flow*, Elsevier.

Choi H. H., Nguyen J. (2016) Numerical investigation of backward facing step flow over various step angles, *Procedia Engineering*. **154**, 420–425.

Durst F., Tropea C. D. (1981) Backward-Facing Step Flows in Two-Dimensional Ducts and Channels, *Proc 3rd Int Symp on Turbulent Shear Flows*, Davis, CA, 1981, 18.11–18.16.

Eaton J., Johnston J. (1981) A review of research on subsonic turbulent flow reattachment, *AIAA Journal*, **19**, 1093–1100.

Estejab B. (2011) An Investigation of the Reynolds Number Dependence of the Near-wall Peak in Canonical Wall Bounded Turbulent Channel Flow.

Gerasimov A. (2006) Modeling turbulent flows with fluent, *Europe*, ANSYS, lnc.

Hossain M. A., Rahman M. T., Ridwan S. (2013) Numerical investigation of fluid flow through a 2d backward facing step channel, *International Journal of Engineering Research & Technology*, **2**, 3700–3708.

Jovic S., Driver D. M. (1994) Backward-facing step measurements at low Reynolds number, Re (sub h) = 5000.

Kaiktsis L., Karniadakis G. E., Orszag S. A. (1991) Onset of three-dimensionality, equilibria, and early transition in flow over a backward-facing step, *Journal of fluid Mechanics*, **231**, 501–528.

Kim J., Kline S., Johnston J. P. (1980) Investigation of a reattaching turbulent shear layer: flow over a backward-facing step.

Krishnamoorthy C. (2007) *Numerical analysis of backward-facing step flow preceeding a porous medium using FLUENT*, Oklahoma State University.

Launder B. E, Spalding D. B. (1972) Lectures in mathematical models of turbulence.

Le H., Moin P., Kim J. (1997) Direct numerical simulation of turbulent flow over a backward-facing step, *Journal of fluid Mechanics*, **330**, 349–374.

Lee T., Mateescu D. (1998) Experimental and numerical investigation of 2-D backward-facing step flow, *Journal of Fluids and Structures*, **12**, 703–716.

Lilly D. K. (1966) On the application of the eddy viscosity concept in the inertial sub-range of turbulence, *NCAR manuscript 123*.

Menter F. R. (1994) Two-equation eddy-viscosity turbulence models for engineering applications, *AIAA Journal*, **32**, 1598–1605.

Mustafa A. M. (2012) The Design of a Program for Open Channel Optimization M.Sc. University of Gaziantep.

Neumann J., Wengle H. (2003) DNS and LES of passively controlled turbulent backward-facing step flow, *Flow, turbulence and Combustion*, **71**, 297–310.

Panjwani B., Ertesvag I., Gruber A., Rian K. E. (2009) Large eddy simulation of backward facing step flow, *5th national conference on computational mechanics*, MekIT09, Trondheim, Norway.

Pont-Vílchez A., Trias F., Gorobets A., Oliva A. (2019) Direct numerical simulation of backward-facing step flow at and expansion ratio 2, *Journal of Fluid Mechanics*, **863**, 341–363.

Qingfu X., Zhiping L. (2012) Study on Flow Reattachment Length, *Procedia Engineering*, **28**, 527–533.

Saad T. (2011) Turbulence modeling for beginners, *University of Tennessee space institute*.

Shehadi E. (2018) Large Eddy Simulation of Turbulent Flow over a Backward-Facing Step.

Shih T.-H., Liou W. W., Shabbir A., Yang Z., Zhu J. (1995) A new k-ε eddy viscosity model for high reynolds number turbulent flows, *Computers & fluids*, **24**, 227–238.

Sinha S., Gupta A., Oberai M. (1981) Laminar separating flow over backsteps and cavities. I-Backsteps, *AIAA Journal*, **19**, 1527–1530.

Smagorinsky J. (1963) General circulation experiments with the primitive equations: I. The basic experiment, *Monthly Weather Review*, **91**, 99–164.

Sobieski W. (2013) Relationships between CFD and experimental fluid mechanics, *Technical Sciences/University of Warmia and Mazury in Olsztyn*.

Tihon J., Pěnkavová V., Havlica J., Šimčík M. (2012) The transitional backward-facing step flow in a water channel with variable expansion geometry, *Experimental Thermal and Fluid Science*, **40**, 112–125.

Wang F.-F., Wu S.-G., Zhu S.-L. (2019) Numerical simulation of flow separation over a backward-facing step with high Reynolds number, *Water Science and Engineering*, **12**, 145–154.

Wilcox D. C. (1998) *Turbulence modeling for CFD*, DCW industries La Canada, CA.

Yakhot V., Orszag S. A. (1986) Renormalization group analysis of turbulence. I. Basic theory, *Journal of Scientific Computing*, **1**, 3–51.

Yüce M. I. (2005) An experimental investigation of pollutant dispersion and trapping in shallow re-circulating flows in harbors and sudden enlargements PhD. University of Manchester.

Zajec B., Matkovič M., Kosanič N., Oder J., Mikuž B., Kren J., Tiselj I. (2021) Turbulent Flow over Confined Backward-Facing Step: PIV vs. DNS, *Applied Sciences*, **11**, 10582.